time from the HPC Department of Defense Shared Resource Center, U.S. Army Corps of Engineers Waterways Experiment Station, Vicksburg, MS, as well as from the Numerical Aerodynamic Simulation facility.

References

[1]Allmaras, S. R., "Contamination of Laminar Boundary Layers by Artificial Dissipation in Navier–Stokes Solutions," Annual Modeling and Simulation Conf., Pittsburgh, PA, April 1992.

[2]Baldwin, B. S., and Barth, T. J., "A One-Equation Turbulence Transport Model for High Reynolds Number Wall-Bounded Flows," AIAA Paper 91-0610, Jan. 1991.

[3]Spalart, P. R., and Allmaras, S. R., "A One-Equation Turbulence Model for Aerodynamic Flows," AIAA Paper 92-0439, Jan. 1992.

[4]Coakley, T. J., and Huang, P. G., "Turbulence Modeling for High Speed Flows," AIAA Paper 92-0436, Jan. 1992.

[5]Bradshaw, P., "Progress in Turbulence Research," AIAA Paper 90-1480, June 1990.

[6]Baldwin, B. S., and Lomax, H., "Thin Layer Approximation and Algebraic Model for Separated Turbulent Flows," AIAA Paper 78-0257, Jan. 1978.

[7]Launder, B. E., and Sharma, B. I., "Application of the Energy Dissipation Model of Turbulence to the Calculation of Flows Near a Spinning Disk," *Letters in Heat and Mass Transfer*, Vol. 1, 1974, pp. 131–138.

[8]Gaitonde, D., and Shang, J. S., "The Structure of a Double-Fin Turbulent Interaction at Mach 4," AIAA Paper 94-2810, June 1994; *AIAA Journal* (to be published).

[9]Gaitonde, D., and Shang, J. S., "On the Structure of an Unsteady Type IV Interaction at March 8," *Computers and Fluids Journal*, Vol. 24, No. 4, 1995, pp. 469–485.

[10]Wideman, J. K., Brown, J. L., Miles, J. B., and Özcan, O., "Skin-Friction Measurements in a Three-Dimensional, Supersonic Shock-Wave/Boundary-Layer Interaction," *AIAA Journal*, Vol. 33, No. 5, 1995, pp. 805–811.

[11]Gaitonde, D., Edwards, J. R., and Shang, J. S., "The Computed Structure of a 3-D Turbulent Interaction Caused by a Cylinder/Offset Flare Juncture," AIAA Paper 95-0230, Jan. 1995.

[12]Edwards, J. R., and Chandra, S., "Eddy Viscosity—Transport Turbulence Models for High-Speed, Two-Dimensional, Shock-Separated Flowfields," AIAA Paper 94-0310, Jan. 1994.

[13]Bradshaw, P., "Turbulence: The Chief Outstanding Difficulty of Our Subject," *Experiments in Fluids*, Vol. 16, 1994, pp. 203–216.

Skewed Shear-Layer Mixing Within a Duct

Thomas F. Fric*
General Electric Corporate R&D Center, Schenectady, New York 12301

Introduction

CASES occur where shear layers are inherently more three-dimensional than nominally two-dimensional mixing layers. The skewed mixing layer, which is formed by two streams at an angle to each other, is one example. Skewed mixing layers can be better mixers than two-dimensional layers,[1–4] and the analysis of Lu and Lele showed that the growth rate of skewed mixing layers can be represented by an effective shear-velocity difference of the two streams.[3]

In the experiments highlighted here, incompressible skewed shear-layer mixing is studied. The mixing region is confined in the sense that the streams impinge somewhat on the side walls of the duct into which the two streams flow. Generally there are differences in the two streams' relative speeds in both the streamwise and spanwise directions, and therefore fluxes of two vorticity components separate from the splitter plate. The mass flow ratio is varied for a fixed amount of skewing, and mixing development within the duct is investigated.

Received Nov. 28, 1994; presented as Paper 95-0869 at the AIAA 33rd Aerospace Sciences Meeting, Reno, NV, Jan. 9–12, 1995; revision received Oct. 27, 1995; accepted for publication Nov. 16, 1995.

*Aeronautical Engineer, Fluid Mechanics Program.

Experimental Setup

Figure 1 shows the two skewed streams, mixing duct, and laser, optics, and camera for the planar laser-induced fluorescence (PLIF) technique. The top and bottom streams are injected at 26 and 13 deg relative to the duct axis, respectively. The splitter-plate trailing edge is located 2.5 cm downstream of the transition between the injected streams and mixing duct. Screens and honeycomb were used to condition the injected streams. The distance from the downstream edge of each stream's flow conditioning to the splitter-plate edge was 47.0 cm, and the boundary-layer momentum thicknesses at the end of the splitter plate were estimated to be in the range of 0.5–1.1 cm, depending upon the mass flow rate. The mixing-duct dimensions are 12.7 cm wide by 9.3 cm high. Further details about the setup are available.[4]

Planar laser-induced fluorescence of fluorescein dye in water was used. All images captured by an 8-bit charge-coupled device (CCD) camera were corrected for laser sheet nonuniformity, background light, and camera response.[5] The laser sheet was steered across the mixing region to reveal cross-sectional images at several duct planes. The CCD camera viewed the mixing process through a window located at the end of the duct, 66.0 cm downstream from the splitter-plate trailing edge.

Table 1 shows flow conditions for five test cases. The bottom-to-top stream mass-flow ratio k defines each test case. High- and low-speed streams are indicated as streams 1 and 2, respectively. By ϕ_1 we denote the skewing angle of the higher-speed stream, and by ϕ_2 the skewing angle of the lower-speed stream, both relative to the duct axis. The total skewness ϕ is given by $\phi_2 - \phi_1$. The Reynolds number, based on duct height h and mean streamwise duct velocity, is 3000.

Results

Figure 2 show streamwise progression of mixing for $k = 2$. Each image shows time-averaged scalar concentrations of 50 instantaneous fields. The gray scale from white (top stream) to black (bottom stream) shows mixture levels between the two streams. At $x/h = 1$, Fig. 2a shows the growth and structure of the interface between the two streams and a counterclockwise rotation of the interface. The thin central portion of the shear layer shows evidence of two streamwise structures with counterclockwise vortical sense, and the bottom left and top right corners show the collection of streamwise vorticity. The top stream fluid, with a velocity component from right to left, impinges on the left duct wall and moves downward. Similarly the bottom stream fluid impinges on the right wall and moves upward, displacing what was initially pure top-stream fluid. Figure 2b shows mixing-layer growth and improvement in mixture uniformity at $x/h = 2$. Figures 2c and 2d show further development

Table 1 Flow conditions

$k \equiv m_b/m_t$	$r \equiv u_2/u_1$	ϕ_1, deg	ϕ_2, deg	$\phi \equiv \phi_2 - \phi_1$, deg
5	0.22	−13	26	39
2	0.54	−13	26	39
1	0.92	−13	26	39
0.5	0.46	26	−13	−39
0.2	0.18	26	−13	−39

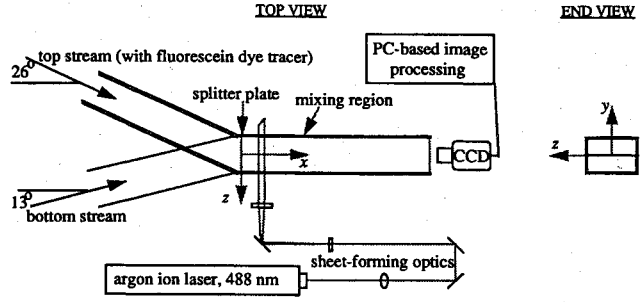

Fig. 1 Schematic of experimental setup.

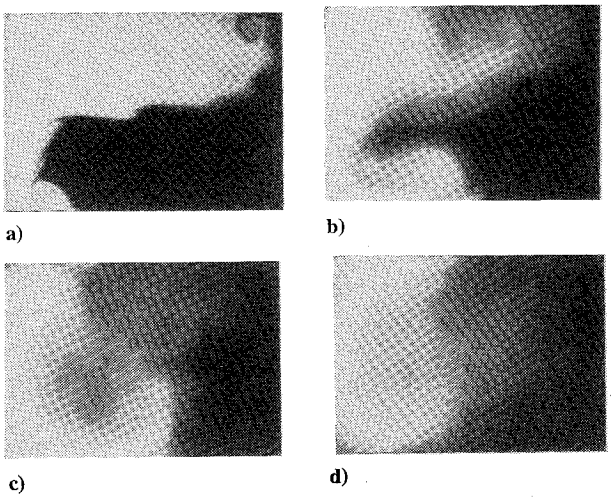

Fig. 2 Scalar concentration PLIF images. Mass-flow ratio $k = 2$: a) $x/h = 1$, b) $x/h = 2$, c) $x/h = 3$, and d) $x/h = 5$.

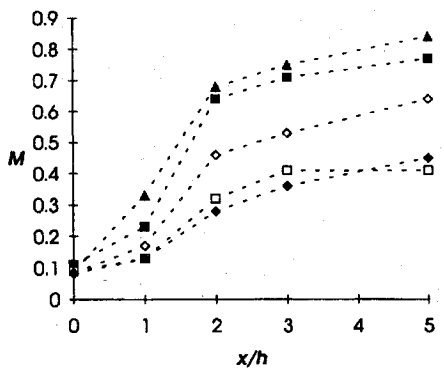

Fig. 3 Skewed shear-layer mixedness M for five mass-flow ratios. (Uncertainty in M is ± 0.1 at 20:1 odds.) --■--, $k = 5$; --□--, $k = 2$; --◆--, $k = 1$; --◇--, $k = 0.5$; and --▲--, $k = 0.2$.

of mixing. There is a general sense that the flow has a counterclockwise rotation from $x/h = 1$ through $x/h = 5$. The images suggest that the interface thickness within this overall motion is governed by the growth of the central portion of the mixing layer. The flow structure observed for $k = 5$, 1, 0.5, and 0.2 is similar to that shown here for $k = 2$. However, the mixture uniformity generally differed among mass-flow ratios.[4]

To track mixing progress quantitatively, a scalar mixedness parameter M defined as

$$M \equiv 1 - \frac{\int (c - C)\,dA}{\left[\int (c - C)\,dA\right]_{x/h=0}} \tag{1}$$

is used, where $c(x, y, z)$ is the scalar concentration of bottom stream fluid, C is its spatial average at a cross section, and $0 \leq M \leq 1$. The case $M = 0$ indicates the totally unmixed initial state, and $M = 1$ indicates the uniformly mixed state where c equals C everywhere at a cross section.

Mixedness parameters for skewed mixing layers at five mass-flow ratios are shown in Fig. 3. It shows values of M near the splitter-plate edge and at four cross sections matching those shown in Fig. 2. The data show that M is a strong function of x/h and k. The largest improvement in mixing occurs within the first two duct heights, and mixing is not complete by $x/h = 5$. At each x/h the mixedness was greatest for $k = 0.2$, followed by $k = 5$. The mixedness was poorest for $k = 1$ and 2. At $x/h = 5$, values of M ranged from 0.41 for $k = 2$ to 0.84 for $k = 0.2$.

From images such as Fig. 2a, effects of k on early mixing-layer growth are identifiable, particularly for the central portion of the interface. M values at $x/h = 1$ correlate well with the visual shear-layer thicknesses.[4] In particular, the visual thickness is smallest for $k = 1$ and is largest for $k = 0.2$. Figure 3 shows that the relative mixedness among the five cases remains the same from $x/h = 1$ through $x/h = 5$. This suggests that the initial shear-layer growth

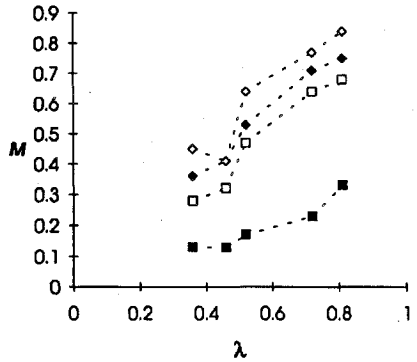

Fig. 4 Dependence of mixedness M on effective growth rate parameter λ. (Uncertainty in M is ± 0.1 at 20:1 odds.) --■--, $x/h = 1$; --□--, $x/h = 2$; --◆--, $x/h = 3$; and --◇--, $x/h = 5$.

rate is instrumental in establishing the overall downstream mixing effectiveness. The additional influence of the streams impacting on the duct sides walls on M, however, is not explicitly known from these data.

The dependence of M on x/h follows a characteristic curve shape, common to each of the five mass-flow ratios. In particular, the slopes of the curves of Fig. 3 start out relatively low between $x/h = 0$ and 1, increase between $x/h = 1$ and 2, and then level out for $x/h > 2$. Figure 3 shows that the mixing is better for $k = 0.5$ and 0.2 than for $k = 2$ and 5, respectively; mixing is improved when the high-speed stream is also the one that is more highly skewed. This observation motivated the application of Lu and Lele's effective-growth-rate scaling.[3] Lu and Lele introduce an effective growth rate $\lambda \equiv \Delta u/u_{cx}$, where Δu is the effective shear velocity (vector magnitude) difference between the two streams, and u_{cx} is the convection velocity of the mixing layer in its growth (x) direction. The z direction is homogeneous, but in the present case it is understood that the development of the flow is affected by the duct side walls. However, since flow visualization shows[4] a dependence of growth rate on k, this application of λ is pursued. From geometry,[4]

$$\lambda = \frac{2(1 - 2r\cos\phi + r^2)^{\frac{1}{2}}}{\cos\phi_1 + r\cos\phi_2} \tag{2}$$

λ incorporates total skewness, velocity ratio, and the streams' relative skew to the splitter plate edge. The value of λ and the maximum amplification rate from linear stability analysis each increase[3] with skew angle for a given velocity ratio r. Figure 4 shows the dependence of mixing effectiveness on λ at four cross sections. The consistent increase of M with λ suggests that λ is a useful parameter for collapsing the combined effects of skewness and velocity ratio. This result is perhaps somewhat surprising, since the effects of duct walls are of course not part of the effective-growth-rate analysis. However, since the early mixing-layer visual growths also correlate[4] with λ, at least part of the effect on mixing appears to be due to the effective shear properties.

This information, along with that of Fig. 3, suggests that the mixing enhancement caused by skewing is predominant within the first couple of duct heights. The differences in overall mixing within the duct appear to be most influenced by the differences in mixing rates early in the mixing process. After two duct heights the mixing rates (slopes of the curves in Fig. 3) are essentially similar and low for all cases. Perhaps the duct walls' influence on mixing is to actually reduce the mixing rate further downstream, as the duct walls' shear effects may reduce rotation initially imparted to the flow by skewing.

Concluding Remarks

These experiments have quantified mixing effectiveness when skewing the streams constituting a mixing layer within a duct. Mixing effectiveness was found to be a strong function of mass-flow ratio, and mixing rates were observed to be greater early in the mixing process. In applications, the mixing enhancement obtained by skewed layers must be weighed by possible side effects (e.g., losses) of injecting the streams in different directions.

Streamwise structure was observed in the initial portion of the mixing layers. However, because of interactions with the walls of the duct, the dominant streamwise structures observed were the collections of vorticity in the corners of the duct. It is not clear from our results what the influence of the corner vortices is on the mixing process. Spanwise vortical rollups, similar to those typically seen in normal mixing layers, have also been observed.[4]

Mixing improved when the stream with greater skew also was the faster stream. An effective-growth-rate parameter λ was applied, and the results suggest that λ is a useful parameter for simultaneously incorporating speed ratio and skew angle into an effective shear.

References

[1]Hackett, J. E., and Cox, D. K., "The Three-Dimensional Mixing Layer Between Two Grazing Perpendicular Streams," *Journal of Fluid Mechanics*, Vol. 43, Aug. 1970, pp. 77–96.

[2]Grundel, H., and Fiedler, H. E., "The Mixing Layer Between Non-Parallel Streams," *4th European Turbulence Conference Abstracts*, Delft Univ. of Technology, Delft, The Netherlands, 1992, pp. 27–29.

[3]Lu, G., and Lele, S. K., "Inviscid Instability of a Skewed Compressible Mixing Layer," *Journal of Fluid Mechanics*, Vol. 249, April 1993, pp. 441–463.

[4]Fric, T. F., "Skewed Shear Layer Mixing Within a Duct," AIAA Paper 95-0869, Jan. 1995.

[5]Van Cruyningen, I., Lozano, A., and Hanson, R. K., "Quantitative Imaging of Concentration by Planar Laser-Induced Fluorescence," *Experiments in Fluids*, Vol. 10, No. 1, 1990, pp. 41–49.

Supersonic Separation with Obstructions

S. B. Verma* and Vijay Gupta†
Indian Institute of Technology, Kanpur 208 016, India

Introduction

THE complex problem of the supersonic flow along a flat plate as it interacts with blunt obstructions has recieved considerable attention.[1,2] The presence of a blunt obstruction in supersonic flow causes the formation of a bow shock wave ahead of the obstruction. The adverse pressure gradient resulting from the bow shock wave propagates upstream in the subsonic flow within the boundary layer and results in the separation of the boundary layer and formation of vortices ahead of the obstruction. These vortices scavenge the boundary layers leading to increased pressures and heat transfer loads.

Various attempts have been made to correlate the separation distance S, which is defined as the distance from the leading edge of the obstacle to the primary separation line, ahead of the obstacle to the height H of the obstacle.[3,4] According to Sedney and Kitchens[5] the most important dimensionless parameters that have significant effect on S/D values are the ratio H/D and Mach number M of the flow. The value of S/D has been observed to increase with M, though the dependence has been found to be weak.[6] A significant effect of H/D on S/D values has been reported. The value of S/D has been observed to increase with increase in H/D values until a point where it approaches an infinite effective height case, after which S/D assumes a constant value, independent of H/D.

Experimental Apparatus and Test Conditions

The experiments were carried out in the 0.18×0.13 m supersonic wind tunnel of the Indian Institute of Technology, Kanpur. This facility is an intermittent, blowdown type wind tunnel. The models used in the present study consisted of obstacles of various sizes (heights H and diameters D) and shapes (circular cylinders and rectangular blocks) mounted on a splitter plate that was carefully aligned with the flow direction (Fig. 1). The leading edge of the plate was made sharp with an angle of 10 deg on the lower side so as to ensure supersonic flow over the plate. The shock wave from the leading edge was seen to be attached and weak enough to be neglected. Thus, the system produced a flow parallel to the plate at the specified Mach number. The plate spanned the width of the tunnel, and the clearance between the plate edges and side walls was sealed using a shaped rubber-gasket mounted flush with the surface. The model protuberances were mounted on the flat plate at two different distances from the leading edge. This enabled experimentation with two different boundary-layer thicknesses.

All of the tests were conducted at a single Mach number value of 1.6 ± 0.1 and at a constant stagnation pressure of 49.0 ± 0.1 psia. The stagnation temperature was fairly constant for all flows, being 13 ± 0.5°C. The unit Reynolds number for the given test conditions was $(3.6 \pm 0.2) \times 10^7$ m^{-1}. Thus, the two test lengths $X_1 = 11 \pm 0.1$ cm and $X_2 = 24 \pm 0.1$ cm gave $Re_{X_1} = (3.97 \pm 0.23) \times 10^6$ and $Re_{X_2} = (8.68 \pm 0.52) \times 10^6$ for the boundary-layer flows. The onset of turbulence usually occurs at length Reynolds number range[7] of 5×10^5–3×10^6. The freestream turbulence in the tunnel used is quite high, of the order of 0.5%. Under such conditions, transition can be assumed[8] to occur at $Re_X = 1.1 \times 10^6$. The length Reynolds numbers obtained in our case, therefore, suggest that the boundary layer can be taken as fully turbulent. The boundary-layer thicknesses are estimated by the procedure suggested by Van Driest[9] for Mach number greater than unity. The corresponding boundary-layer thicknesses, therefore, turned out to be $\delta_{X_1} = 2.0 \pm 0.1$ mm and $\delta_{X_2} = 3.7 \pm 0.1$ mm. The uncertainty in measurement of quantities such as Y, D, and S is ± 0.1 cm.

Results and Discussions

Figure 2 shows the typical flow pattern as developed from the surface flow studies. These surface flow patterns reveal a primary separation line as observed by Ozcan and Holt[10] in the Reynolds number range of 10^6. Immediately behind the primary separation line, the flow in front of the obstacle is radially outward but becomes largely circumferential away from the medial line. One important feature not referred to by any observer is a thick pigment line running parallel to the primary separation line. This can be termed as a neck compression shock, representing the coming together of streamlines because of the limited side flow/pressure relief afforded by the three-dimensional nature of the obstruction. For obstacles of large heights, a reattachment line was observed very close to

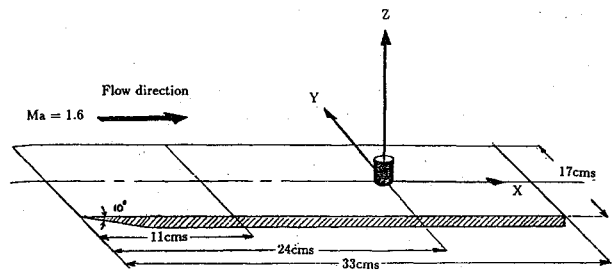

Fig. 1 Isometric view of the plate model.

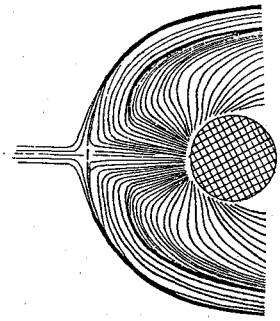

Fig. 2 Typical flow pattern as developed from surface flow studies.

Received Dec. 10, 1994; revision received March 25, 1995; accepted for publication June 12, 1995.

*MTech Student, Department of Aerospace Engineering.
†Professor, Department of Aerospace Engineering.